RADIO-LOUD CME-CME POTENTIAL INTERACTIONS IN SOLAR CYCLE 24 IN THE YEARS 2009-2018

By

Mebrahtu Gebremedhin Teka

Supervisor:Tsega Berhane Teklu (Ph.D) ,in Astro physics:

SUBMITTED IN PARTIAL FULFILLMENT OF THE
REQUIREMENTS FOR THE DEGREE OF
MASTER OF SCIENCE IN ASTROPHYSICS
AT
MELELLE UNIVERSITY
MEKELLE , ETHIOPIA
DECEMBER 2024

MELELLE UNIVERSITY
DEPARTMENT OF
PHYSICS

The undersigned hereby certify that they have read and recommend to the Faculty of COLLEGE OF NATURAL AND COMPUTATIONAL SCIENCES for acceptance a thesis entitled "**Radio-Loud CME-CME Potential Interactions in Solar Cycle 24 in the Years 2009-2018**" by **Mebrahtu Gebremedhin Teka** in partial fulfillment of the requirements for the degree of **Master of Science in Astrophysics**.

Dated: December 2024

Supervisor: _____
Supervisor:Tsega Berhane Teklu (Ph.D) ,in Astro physics

Readers: _____
External Examiner

_____
External Examiner

MELELLE UNIVERSITY

Date: **December 2024**

Author: **Mebrahtu Gebremedhin Teka**

Title: **Radio-Loud CME-CME Potential Interactions in Solar Cycle 24 in the Years 2009-2018**

Department: **Physics**

Degree: **M.Sc.** Convocation: **December** Year: **2024**

Permission is herewith granted to Melelle University to circulate and to have copied for non-commercial purposes, at its discretion, the above title upon the request of individuals or institutions.

Signature of Author

To Physics Teachers.

Table of Contents

List of Tables

List of Figures

Acronyms

AU⇒Astronomical Unit

C2⇒Telescope 2 in Large Angle and Spectrometric Coronagraph (on SOHO)

C3⇒Telescope 3 in Large Angle and Spectrometric Coronagraph (on SOHO)

CDAW⇒Coordinated Data Analysis Workshop

CME⇒Coronal Mass Ejection

COR1⇒Coronagraph 1 (on STEREO)

COR2⇒Coronagraph 2 (on STEREO)

D⇒Decametric

DH⇒Decameter-Hectometric

EIT⇒Extreme-ultraviolet Imaging Telescope (on SOHO)

EUVI⇒Extreme Ultraviolet Imager (on STEREO)

FOV⇒Field of View HI1!Heliospheric Imager 1 (on STEREO)

HI2⇒Heliospheric Imager 2 (on STEREO)

H-T⇒Height-Time

ICME⇒Interplanetary Coronal Mass Ejection

IP⇒Interplanetary

LASCO⇒Large Angle and Spectrometric Coronagraph (on SOHO)

MHD⇒Magnetohydrodynamic

MHz⇒Mega Hertz

NASA⇒National Aueronautics Space Administration

NOAA⇒National Oceanic and Atmospheric Administration

OSO-7⇒Seventh Orbiting Solar Observatory

pB⇒Polarization Brightness

Pri-CME⇒Primary Coronal Mass Ejection

Pre-CME⇒Preceding Coronal Mass Ejection

Rs⇒Solar radius

SECCHI⇒Sun Earth Connection Coronal and Heliospheric Investigation

SOHO⇒Solar and Heliospheric Observatory

SSN⇒Sunspot Number

STEREO⇒Solar Terrestrial Relations Observatory

STEREO-A⇒STEREO Ahead

STEREO-B⇒STEREO Behind

WAVES⇒Radio and plasma wave experiment (on board wind)

Wind⇒NASA'S sattelite

TRACE⇒Transition Region and Coronal Explorer

SMM⇒Solar Maximum Mission

ESA⇒European Space Agency

Abstract

Radio loud (RL) CMEs are those associated with solar type II radio bursts. These CMEs might interact with each other on their way from the solar surface to the interplanetary medium. As a result ,these CMEs leave a radio signature on the dynamic spectrum and bright white enhancement on the white-light images. In this research ,we have found a total set of 32 possible interacting CMEs and 16 associated DH type II bursts are registered on the NASA SOHO/LASCO CDAW catalogue for the period spanning from 2009 to 2018. However , only the DH component of the radio bursts were considered. This possibility of interaction was estimated by a thorough investigation of the origins of the CMEs and the simultaneity of enhancement on the CMEs difference images on the LASCO field of view and the intensification of the burst on the dynamic spectrum of the Wind/WAVES. A primary CME is mainly emitter of the DH burst and the preceding interacts with it. By tracking the white-light images of these CMEs ,the height-time diagrams are obtained. Our results show that most of the primary CMEs are halo and averagely much faster (1482.3 kms^{-1}) than the preceding CMEs (841.6 kms^{-1}). More over ,drift rate of DH type IIs ,time duration of pre and pri-CMEs and interaction height are found to be 1.82 $MHzs^{-1}$, $\sim$34.6 min and $\sim$5.3 Ro ,respectively. The pre-CMEs are found to be less energetic than the primary CMEs. Most of the interacting CMEs were originating from the western regions of the Sun. Studying the properties of interacting RL CMEs and their kinematics are important to be able to make predications before a CME arrival and make proper arrangements both on the ground and in space.

Keywords : RL CMEs , DH type II Bursts , CME-CME interactions ,and SC 24

Acknowledgements

This thesis is the result of my long journey in receiving my MSc. Above all ,I give special thanks to my Father ,Son of God. I would like to thank Dr.Tsega Berhane my supervisor ,for her many suggestions and constant support during this research. I am also thankful all the instructor who have given me the M.Sc courses. I am grateful to acknowledge MOE and Tigray region for giving me this chance and supporting me to learn and also thanks to Mekelle University for providing partial financial support for the completion of my studies and accepting me to continue my study. I am gratefully acknowledging CDAW NASA ,World Data center and the authors of research journals publications and books. Finally ,I am grateful to my wife for her understanding,endless patience , encouragement and support for the successful completion of this work.

Mekelle,Ethiopia
December 30,2024

Mebrahtu Gebremedhin

Chapter 1

Introduction

1.1 Background of the study

The sun has played a dominant role since time of immemorial for different natural activities in the universe at large and in the Earth in particular for the formation of solar activities such as solar flares ,coronal mass ejection ,high speed solar wind and solar energetic particle events. Generally the Sun is the energy source for our planetary system ,which the life on our planet Earth solely depends up on the energy producing from the sun. In this chapter , we begin with the basic concept of the Sun ,its structure , Interplanetary medium ,Solar Eruptive Phenomena ,instrumentations , Solar cycle 24 ,CME-CME interactions ,and Objectives are discussed. Finally ,Statement of the problem ,and rationale of the thesis followed.

1.1.1 The sun and its structure

The Sun is an ordinary star , the nearest to us and the source of heat which sustains life on Earth and controls both terrestrial and space weather. The following are the main physical characteristics of the Sun , as adapted from[2, 3].

- Mass=$(1.9889 \pm 0.0003) \times 10^{30}$kg
- Radius , Rs=$(6.959 \pm 0.007) \times 10^{8}$m (Solar Radius=Rs)
- Age=4.6×10^{9}years
- Chemical composition = hydrogen(92.1%),helium (7.8%)
- Volume=1.412×10^{27} m^3
- Luminosity=3.86×10^{26}W
- Equatorial period of rotation $\sim$27 days
- Surface temperature (photosphere) = 5785K (1.56×10^{7}K in Suns centre and about 2×10^{6}K in the corona)
- Density (centre)=1.513×10^{5}kgm^{-3}
- Pressure (centre)=2.334×10^{16}Pa

The sun was born about 4.6 billion years ago from the gravitational collapse of a vast cloud of gas and dust due to the nuclear fusion of hydrogen at its core. The energy produced from this fusion resulted in enough pressure to counteract gravitational contraction and bring about a hydrostatic equilibrium ,allowing the young star to reach a stability that is sustained to day. The energy released during this process is the ultimate source of light and all energetic activity that we observe from Earth. It is also the largest object in our Solar system and contains approximately 99.8% of the total Solar system mass. The solar mass is strongly concentrated to wards the center. The Sun is also a living ,dynamic star with varying activity. Changes in solar activity

result in many important phenomena in the space environment ,ranging from solar flares ,to coronal mass ejections ,to geomagnetic storms [4]. The structure of the Sun can be broadly divided into two parts:the solar interior and the solar atmosphere. The interior part consists of the core ,radiation zone ,and convective zone (see Figure 1.1. Its solar atmosphere comprises of the photosphere ,chromosphere transition region ,and corona. The solar atmosphere is mostly dominated by magnetic fields ,which are produced in the solar interior at the base of the convection zone.

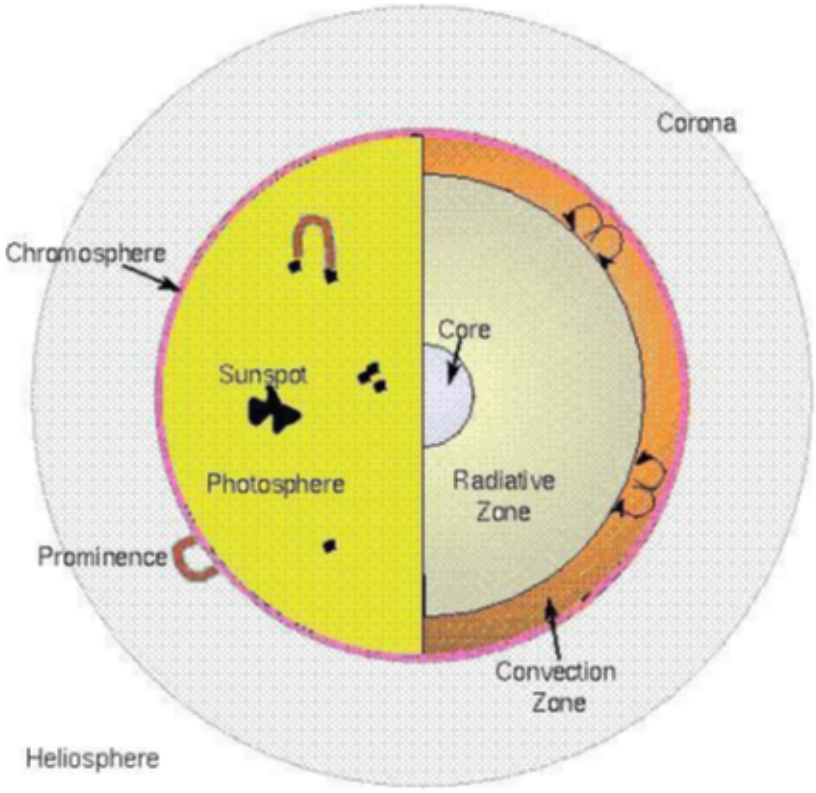

Figure 1.1: Sketch of the Sun's structure.

Based on energy propagation mechanisms the Suns interior is classified into core ,radiation zone and convection zone. The core(at the center of the sun) is the high density ,high temperature region at the center of the Sun(ranges b/n 1.5×10^7k and

160gcm^{-3} at the center to 7×10^{16}k and 20gcm^{-3} at the outer edge of the core) ,where thermonuclear energy production takes place through fusion. The core extends from the center up to 0.25 Rs of the solar radii ,but it contains about half of the solar mass [5]. The radiative zone is a region of highly ionized gas and extends from (0.25 to 0.7) Rs. In this zone the material gets cooler from (7 to 2) million Kelvins with increasing altitude. The energy produced in the core is transported through the core and the radiative zone by gamma ray diffusion. A transition zone ,called the tacho cline , exists between the radiative and convective zone above it. The tacho cline is most likely the location where the solar magnetic field is created [5]. Above the radiative layer is the convective layer where the temperature is lower ,and radiation is less significant. Energy is transported outward mostly by convection. This zone is located in the upper most 30 % (which extends from (0.7 to 1) Rs of the solar interior. In this region the solar material is convectively unstable ,because the radial temperature gradients are large. The temperature drops from 2,000,000 Kelvins to about 6000K on the outer layer and it is less dense than the core and the radiative zone ,which allows the easy upward motion of the plasma and heat to the photosphere. Convective circulation of plasma (charged particles)generates large magnetic fields that play an important role in producing sunspots and flares [6]. Based on the temperature or density profile ,the solar atmosphere can be divided in to four regions,Photosphere ,Chromo sphere,transition region,and Corona. The lowest atmospheric layer ,called the photosphere,is an extremely thin and visible surface layer of the Sun where most photons interact with atoms a last time before escaping from the Sun ,and its temperature ranges from 6400 to 4400 K thickness and the electron density of the photosphere are 500 km and 10^{19}-10^{21}m $^{-3}$,respectively [7].

The photosphere is covered by granulation ,brighter regions separated by darker edges ,are observed in the photosphere which represents the tops of convective cells rising from the interior. Two or three characteristic cell sizes can be distinguished:granules are bright features of order of hundreds to a thousand km across , with life times of about (5 to 10) minutes ,surrounded by dark edges ,representing the down flow of convection cells ,super granules are of order of 30,000 km across ,with life times of 12 to 24 hours. The photosphere rotates with a higher speed at the equator than at the polar region despite the rigid motion of the core and the radiative zone. However ,over small fractions of the solar surface ,the granulation is replaced by sunspots usually surrounded by a filamentary penumbra. They are regions where strong magnetic field is concentrated. Sun spots are formed when magnetic flux tubes just below the Suns surface are compressed by the subsurface plasma pressure and poke through the solar photosphere. They are somewhat cooler (4,000 K) than the average surface(6,000K) , and so they appear darker by comparison. It is observed that sun spots often come in pairs , with opposite magnetic field polarity [8, 9]. At these higher temperatures hydrogen emits light that gives off a reddish color (H-alpha emission). This colorful emission can be seen in prominences that project above the limb of the sun during total solar eclipses. This is what gives the chromosphere its name (color sphere). The layer between the relatively cool chromosphere and the hot corona is called the transition region. The transition region is a very thin layer of the Suns atmosphere ,just above the chromosphere ,a relatively small regime of few hundred kilometers(about 500 km). This region is locally visible by space telescopes in the UV (ultraviolet)range. Analysis of both solar ultraviolet and radio observations have shown the existence of a steep increase of temperature within transition

region. This region is an important chromosphere-corona boundary over which the temperature rises drastically from 20,000 Kelvin in the upper chromosphere to over 2 million degrees Kelvin in the corona. Most of the transition region emission occurs in the VUV(vacuum ultraviolet) range of the electromagnetic radiation[10].

The corona is the outer most part of the Suns atmosphere. It can clearly be seen during the total solar eclipse as a bright region that extends more than some solar radii away from the disk of the sun. The corona is not always evenly distributed across the surface of the sun. During the Suns active periods ,the corona is distributed over the equatorial and polar regions ,though it is most prominent in areas with sunspot activity. The solar corona is structured by the coronal magnetic field which is rooted at the solar surface and is partially open to the hemisphere. Its magnetic fields have generally very complex structure depending on the solar activity cycle. The outer boundary of the corona is not precisely defined. Its outer boundary may be placed at a distance of from (2 to 3) Rs above the solar surface where the magnetic field lines are dragged out by the solar wind and bent into radial direction. There are two different magnetic zones in the solar corona that have fundamentally different properties : open-field and closed-field regions. Open-field regions connect the solar surface with the interplanetary field and are the source of the fast solar wind[11]. The solar temperature ,density and ionization fall from the core to the chromosphere but then the temperature suddenly increases to millions of Kelvin in the corona (see figure1.2. This sudden increase in temperature is known as the Coronal Heating Problem. The extension of the outer corona beyond$\sim$3 Rs is called the interplanetary (IP) medium[6]. The region between the sun and the planets has been termed the interplanetary medium. Some of the special features in the corona are active regions and

coronal holes. Active regions are localized ,transient volumes of the solar atmosphere that include pages ,sunspots ,faculae ,flares ,and CMEs originate. The sun spots are the photospheric signatures of active regions. Coronal holes are dark regions of the corona in extreme ultraviolet and soft X-ray images.

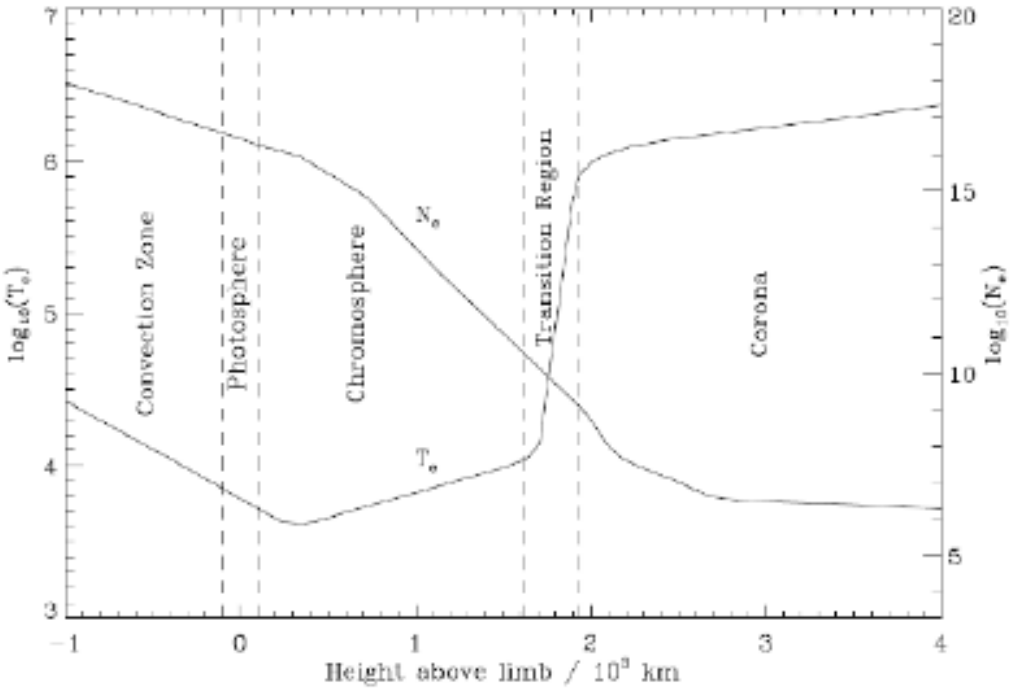

Figure 1.2: The temperature and density profile of solar atmospheres, shows as the height increases the temperature increase and the density is decrease with height taken from[1].

1.2 Interplanetary medium

Nearly all the solar system by volume appears to be an empty void. Far from being no things , this vacuum of space comprises the interplanetary medium. It is an extension of the outer corona beyond ∼3Rs. It includes various forms of energy and at least

two material components : interplanetary dust and interplanetary gas. Interplanetary dust consists of microscopic solid particles. Interplanetary gas is a tenuous flow of gas and charged particle, mostly protons and electrons plasma which stream from the sun , called the solar wind [12].

1.3 Solar activities

The sun is the richest sources of electromagnetic energy (mostly in the form of heat and light) in the solar system. The surface of the sun is a very busy place. It has electrically charged gases that generate areas of powerful magnetic forces ,these areas are magnetic fields. The suns gases are constantly moving which tangles stretches and twists the magnetic fields ,and this motion creates a lot of activity on the suns surface which is called solar activity [12]. The solar activity can have an effect on Earth which is one of the most significant events takes place in the climate of the solar system which is unpredictable. Solar activities includes solar flare ,coronal mass ejections ,high speed solar wind ,and solar energetic particles. All solar activities are driven by the changes occur in the solar magnetic field. The heightened magnetic activity associated with sunspots can lead to solar flare,coronal mass ejection and other far reaching electromagnetic phenomena that endanger astronauts and damage or disrupt satellites[13].

1.4 Solar Eruptive Phenomena

The term solar eruption refers to the sudden release huge amount of energy ,in the inner hemisphere in the form of flares , CMEs , prominence eruption ,energetic particle ,and shock waves.‘The energy is stored in the coronal magnetic fields and released due

to some kind of a trigger ,which is not fully understood[6]. Solar flares and CMEs are the most eruptive phenomena in the solar system. During these explosions ,the emitted radiation and particles can lead to disturbances in the Earth-space environment. Both flares and CMEs are believed to be the result of an explosive release of energy from the active regions in the solar outer atmosphere[14]. Coronal Mass Ejections are literally ejections of mass from the Suns corona. They occur when large scale magnetic fields break and release energy and enormous amounts of matter into space. The matter and magnetic fields from Coronal Mass Ejections (CMEs)travel faster than the solar wind ,but slower than the speed of light. A large CME can contain 10^{16} grams (a billion tons) of matter that can be accelerated to several million miles per hour in a spectacular explosion. CMEs represent large scale and energetic solar eruptions that serve as the primary drivers of geomagnetic storms and other space weather disturbances on Earth. It takes from one to five days to reach Earth[15].

1.5 Solar cycle 24

Solar cycle 24 ,which spanned from approximately 2008 to 2019 ,was noted for its relatively low solar activity compared to previous cycles. Despite this ,several significant CME-CME interaction events were recorded ,providing a unique opportunity to study these interactions under different solar conditions[16]. Research by [17] indicated that the reduced solar activity did not diminish the complexity or impacts of CME interactions during this cycle. Solar cycle 24 is the most recently completed solar cycle,the 24^{th} since 1755 ,when extensive recording of solar sunspot activity began. Astronomers have noticed that the sunspot cycle relates to activity on the Sun ,including powerful coronal mass ejections ,the size and extent of the outer reaches the

Sun (the corona),and the intensity of light and exciting particles the Sun discharges out into the Solar system and space.

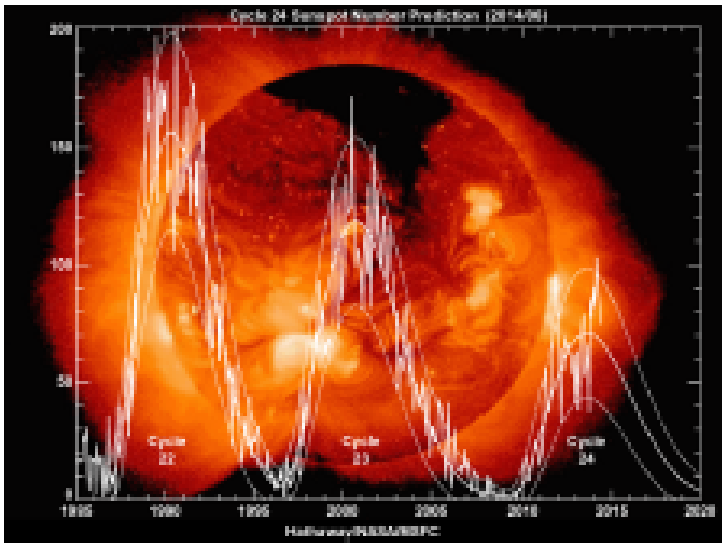

Figure 1.3: The SC,1995-2015.The curve traces measured SN,the smoothed curves are predictions. Credited:D.Hathaway/NASA/MSF

1.6 CME-CME Interactions

CME-CME interaction is a physical process occurring in the interplanetary medium as observed by coronagraphs of SOHO/LASCO [18] and of STEREO [19]. In an interacting event ,a slow CME (called a pre-CME) is followed by a fast CME called as pri-CME from the same/near by active region [20]. The kinematical behavior of isolated CMEs can differ strongly in comparison to a series of CMEs. Successive eruptions from the sun cause a change in interplanetary environment(eg., density and speed) and complex magnetic structure may form during CME-CME interactions observable features CME-CME interaction are restricted to white light and radio data.

The CME kinematics is found to clearly change during the collision of CMEs ,resulting in either strong deceleration [19] or acceleration ,super elastic collision). Correspondingly ,the interaction features may be detected in the WAVES dynamic spectrum at Decameter Hectometric (DH) wavelength as radio enhancement signatures[19].

1.7 Large Angle Spectrometric Coronagraph (LASCO) onboard the Solar Heliospheric Observatory (SOHO)

The Solar Heliospheric Observatory (SOHO) spacecraft was launched on 1995 December 2 with the Large Angle Spectrometric Coronagraph on board. SOHO is located about the ecliptic plane at 0.99 Astronomical Unit (AU) on a halo orbit around the Lagrangian L1. The Solar and Heliospheric Observatory ,is a project of international collaboration between ESA and NASA to study the Sun from its deep core to the outer corona and the Solar wind. SOHO has studied the Sun Earth interaction since 1995. The LASCO instruments originally included three coronagraphs namely C1 ,C2 and C3. However ,the C1 stopped working in 1998. The field of view(FOV) of the C2 and C3 ranges from 2.1 to 6.0 and 3.7 to 32 Rs respectively. A coronagraph is like any other telescope ,except it has an occulter(a disk)that blocks the bright photospheric light from entering the telescope. This allows us to clearly image the much fainter solar corona. The large disk (the occulter) , which blocks the photospheric light,is kept in place by the occulter pylon. The size of the Sun is indicated by the white circle drawn on the occulting disk. Coronal streamers and stars are observed as white light enhancements over the blue back ground[21].

1.8 Sun Earth Connection Coronal and Heliospheric Investigation (SECCHI) on board the Solar Terrestrial Relations Observatory (STEREO)

The twin spacecraft of Solar Terrestrial Relations Observatory were launched in 2006. The two spacecraft started orbiting the Sun near Earth at heliocentric distances of 0.9 and 1.2 AU ,respectively. Because their radial solar distances are different ,they have different orbital speeds ,which cause them to drift away from Earth by 22^0 each per year. The leading and trailing STEREO compared to the Earth are called STEREO Ahead (STEREO A) and Behind (STEREO-B) , respectively[22]. The Sun Earth Connection Coronal and Hemispheric Investigation is a suite of instruments onboard STEREO. SECCHI has 5 different imaging instruments which image the solar disk and the corona from the Sun all the way to 1 AU [23]. These instrumentsare the Extreme Ultraviolet Imager , Coronagraph 1 (COR1),Coronagraph 2 (COR2) , Heliospheric Imager 1 (HI1) and Heliospheric Imager 2 (HI2) with FOVs 1-1.7 , 1.5-4 , 2.5-15 , 15-84 and 66-318 Rs , respectively. The large FOV of the SECCHI helps us to observe a CME at the distances corresponding to long wavelength radio emissions.

1.9 Objective

1.9.1 General objective of the research

•To investigate the characteristics of Radio-Loud CME-CME potential interactions in solar cycle 24.

1.9.2 Specific objectives:

•To identify the possible CME-CME interaction events in SC 24

- •To determine the radio-loud kinematic properties of Pri and pre-CMEs
- •To identify the source location of pri and pre-CMEs
- •To study the frequency ranges of DH type II Burst and drift rates .
- •To verify the time duration and interaction height of pri and pre-CMEs.

1.10 Statement Of problem

CMEs are significant solar phenomena that can impact space weather and technology on Earth. During Solar Cycle 24 ,the occurrence of radio loud CMEs which produce intense radio emissions such as type II bursts has been of particular interest. These CMEs can interact with other CMEs which created complex shock structures and potentially altering their trajectories and speeds. When two or more CMEs are interacting to each other ,the resulting dynamics can be complex and then lead to increase enhanced geomagnetic storms , particle radiation ,and other space weather effects. Understanding the properties and out comes of CME-CME interactions is crucial for predicting their impact on Earths magnetosphere and for mitigating potential disruption to satellite operations,communication systems , and power grids. Despite extensive research on CMEs ,specially radio-loud CMEs ,remain poorly understood. This study aims to fill this gap by investigating the potential interactions b/n radio-loud CMEs during Solar Cycle 24 and their impacts on space weather. All successive disk event CMEs released from the same active region in closed interval time produce geo effective solar storms. These events damage out space and ground-based modern technology like satellite,GPS,aircraft and navigation. These particles also produce

ground induced current (GIC) which burn out our transformer and pipeline of oil and gas as well can affect human life by exposing into hazardous radiation[24].

1.11 Rationale of the study

Understanding the dynamics of radio-loud CMEs and their interactions helps in predicting space weather events,which can affects satellite operations,communication systems,and power grids on Earth[25, 26]. By elucidating how these CMEs influence geomagnetic storms ,the study contributes to better preparedness and response strategies for mitigating the adverse effects of space weather. There are various primary cosmic rays that originated from the Sun and another galaxy that can result in space weather storms and geomagnetic storms. Especially ,out bursts from huge explosions on the Sun generate X-ray Solar Flares and large Coronal Mass Ejections (CMEs)interaction. These events send out space weather rain storms out ward to earth through the solar wind. The Sun emits extreme solar energetic particles or solar cosmic rays in the form of charged particles and comes along the heliomagnetic field that makes up the plasma of the solar wind strong. As a result ,the Sun activities can cause space weather storms that affect ground and space based technologies as well human life on Earth. Thus ,studying of CMEs interaction is helpful to protect space weather events by giving official information for civilian alerts and warnings. Comprehensive understanding of the CMEs interaction can help to minimize ground and space based multiple vulnerabilities of technologies or infrastructures. All in all ,there is no country which is developed without space and ground based technologies ,therefore ,we should have protected and minimized severe geomagnetic storms and space weather events in order to have free space weather ,to monitor high cost

outcomes , to give warnings for operators (aviation,GPS ,spacecraft and others) and to avoid natural hazardous radiation in human health. Therefore ,space weather warnings ,further information in space weather events and CMEs interaction are very important for Ethiopia Space Science Society future development.

Chapter 2

LITERATURE REVIEW

2.1 Coronal mass ejections(CMEs)

Coronal mass ejections are a large expulsions of plasma and magnetic field from the sun corona ,that were first discovered on 1971 December 14 and later on 1972 February 8 using the white light coronagraph aboard NASAS Seventh orbiting solar Observatory(OSO7) [3]. However ,it was in 1973 that the Sky lab clearly identified a CME. Since then various missions , including the Solar Maximum Mission (SMM) ,the Solar and Heliospheric Observatory (SOHO) as well as the recent Transition Region and Coronal Explorer (TRACE) and the Solar Terrestrial Environment Observatory(STEREO) mission launched in 2006 ,have allowed reliable observations and provided more information and knowledge about the morphology and properties of CMEs. The SOHO spacecraft is a NASA/ESA joint project. The LASCO instrument aboard SOHO has 3 coronagraphs (C1 , C2 and C3) that have operated since 1996 and detected more than 10 ,000 CMEs during Solar cycle 23 [27]. CMEs are detected in visible light observations of the solar corona from spacecraft. The coronagraphs image of the CMEs in Thomson scattered photospheric light by blocking the direct

sunlight with an occulting disk [27]. Mass ejections are seen as bright moving loop like features in the corona ,blasting out from the edge of the occulted photosphere. Therefore ,details of the source region are usually obtained using non coronagraphic observations such as in X-rays ,EUV ,microwaves ,and Halpha[28]. A typical CME is mainly characterized by a three part structure , namely:the leading bright edge followed by the dark cavity (or void region) and the bright core. Where the bright leading edge is interpreted as coronal plasma pileup ,the cavity as the magnetic field dominated region and the bright core as the eruptive prominence. This configuration is therefore often viewed as a standard CME in both observational and theoretical studies[29].

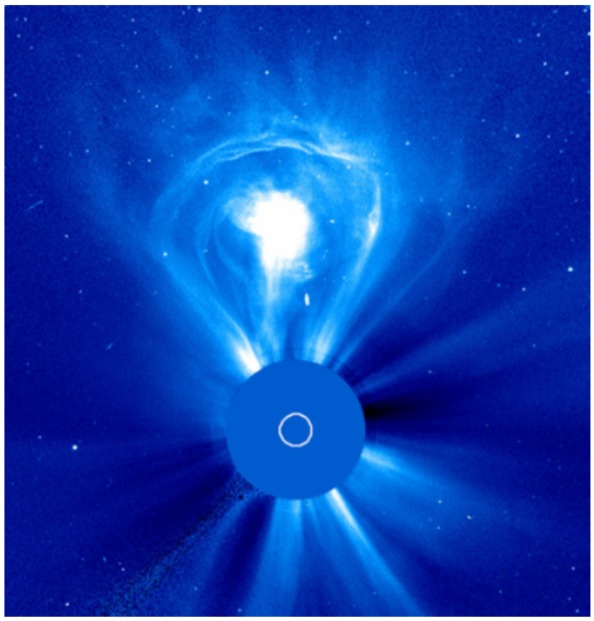

Figure 2.1: white-light coronagraphs on board the SOHO (Solar and Heliospheric Observatory) satellite. Dense plasma structures in the corona become visible via photospheric light Thomson-scattered off the free electrons in the plasma, in the color-scaled image. A typical CME consists of three parts: a cavity of low electron density,a dense core embedded in this cavity, and a bright leading edge.

2.2 Properties of Coronal mass ejections

It is believed that CME is ejected in different shapes ,sizes and much of varieties are due to the projection effect. The main parameters for CMEs identification are its geometry (position angle at the sky plane ,angular width) ,morphology (three part structure, flux rope) ,kinematics (time-distance plots ,speed , acceleration) ,mass ,kinetic energy and its magnetic properties (helicity ,orientation of the magnetic field to wards the earth field). CME undergoes a multi phase kinetic evolution with varying features when goes through corona and inner hemisphere. CMEs appear as large scale coherent structures in corona graphic field of view and show clear outward motion from the Sun. For slow CMEs ,one can often see three part structure consisting of a bright front followed by a dark void and a bright core. The dark void has been interpreted as a magnetic flux rope. The bright core is the eruptive prominence. Fast CMEs often show a structure surrounding the bright front , which is interpreted as the compressed shock sheath ahead of the CME. The shock structure may be useful in measuring the hemispheric magnetic field [30]. Speed ,angular width , and acceleration are considered to be the basic attributes of a CME measured from a series of images taken during an eruption The speed measured in the sky plane varies from 20 kms^{-1} to $>$ 3000 kms^{-1} with an average value of 470 kms^{-1}. The highest speed recorded is 3387 kms^{-1} for a CME on 2004 November 10. The CME width (W) ranges from 5^0 to 360^0. Widths down to 2^0 are measured , but many such narrow CMEs might have been missed especially during the solar maximum [31]. Each CME is characterized by three speeds:(1) the linear speed obtained by fitting straight line to the height-time measurements made at the fastest section of CMEs ,(2) quadratic speed obtained by fitting a parabola and evaluating the speed at the

time of final height measurement ,and (3) speed obtained as in (2) but evaluated when the CME is at a height of 20 Rs. Acceleration is obtained from the quadratic fit to the height time measurement. The derived acceleration generally depends on the initial speed (or its square) with in the corona graphic field of view. All CMEs have positive acceleration in the beginning as they lift off from rest[32]. The angular width is measured as the position angle extent of the CME in the sky plane ,so only those CMEs that are in the sky plane (solar source near the limb) will yield the true width. CMEs that appear to surround the occulting disk of the observing coronagraphs in Sky plane projections are known as halo CMEs. Depending on their width ,CMEs are categorized as non halo ,Partial halo ,and full halo. Full halos have an apparent width(W) of 360^0 ,while partial halos have $120^0 \leq W < 360^0$,and non halo have $<120^0$. Halo CMEs are said to be front sided if the site of eruption (also known as the solar source) can be identified on the visible disk usually identified as the location of H-alpha flares or filament eruptions. Halos with their solar sources within 45^0 of the central meridian are known as disk halos ,while those with a central meridian distance (CMD) beyond 45^0 but not beyond 90^0 are known as limb halos (non disk). Disk halos are likely to arrive at Earth and Cause geomagnetic storms ,while limb halos only impact Earth with their flanks and hence are less. Halo CMEs are more energetic with (average speed is$\sim$1000 kms^{-1} compared to $\sim$470 kms^{-1} for ordinary CMEs[33, 34].

2.2.1 Solar Source of CMEs

Most CMEs originate from active regions , particularly those with sun spots ,which are areas of intense magnetic activity. Those regions are often found in the solar photosphere and are characterized by strong magnetic fields that can lead to magnetic reconnections ,facilitating CME eruptions [35]. Some CMEs can also emanate from coronal holes ,which are areas where the solar corona is less dense and cooler than surrounding regions. These holes are associated with open magnetic field lines and allow for the escape of solar wind and plasma [36]. Many CMEs are linked to solar flares ,particularly X-class flares. The explosive energy released during flares can propel material in to space ,forming CMEs. Studies have shown a strong correlation b/n flare intensity and CME speed [37]. The location of CME sources varies with cycle. During solar maximum ,CMEs are more frequently observed at lower latitudes($\pm$30degrees) ,while during solar minimum ,they can occur at higher latitudes [38]. CMEs occur from closed magnetic field regions ,where magnetic free energy is stored and released during eruptions. A closed field region can be a simple dipole ,an active region ,or a quiescent filament region. In photospheric magnetograms ,all these Regions show positive and negative polarity patches and it is expected that field lines connect from the positive part to the negative part. There is a polarity inversion line ,also known as the neutral line ,where the line of sight field vanishes. A dark filament Often overlies the neutral line and becomes part of the CME (prominence core) when the region erupts. CMEs observed at 1 AU by multiple spacecraft have revealed that the legs of the CME are probably connected to the Sun ,with their feet anchored on either side of the magnetic neutral lines. However ,filaments near coronal holes seem to have a proclivity for eruption[39, 40] which means such eruptions can be mistakenly

associated with coronal holes. Closed magnetic structure ,thus seems to be the basic characteristic of CME producing regions on the Sun ,which means the energy needed to carry billions of tons of ionized plasma in to the hemisphere must ultimately come from the magnetic field itself. How this energy is stored in the coronal magnetic fields and what triggers the energy release are topics of current research and debate.

2.3 Interaction of CMEs

2.3.1 Observation of CME-CME interaction in the Solar Corona

Interaction b/n CMEs occurred when two or more CMEs propagate in the same direction and collide or merge to each other. Thus interactions can lead to complex phenomena that enhance space weather effects. When CMEs interact ,the resulting shock wave can be significantly stronger than those produced by individual CMEs. Enhanced shock strength can accelerate particles to higher energies ,leading to more intense space weather events [41]. CME-CME interaction can amplify radio emissions , particularly type II radio bursts. These amplified emissions are generated by shock waves produced during interaction and can provide valuable information about the dynamics of the interaction [42]. Interactions b/n CMEs can lead to prolonged geomagnetic storms. When a faster CME over takes a slower one ,the combined structure can sustain geomagnetic activity for a longer duration that causing extended disruptions to Earths magnetosphere [43]. As mentioned earlier ,there were about 6 solar eruptions a day during the last solar maximum. The typical propagation time of a CME from the Sun to the Earth is (2.5-3) days. Therefore ,near solar maximum there is a high probability that multiple CMEs will interact on their way to Earth.

Homologous eruptions provide a good example of potential interactions of CMEs on their way to Earth. The smallest delay found between two ejections from the same active region is 2 hours(January 20,2001) , but a delay of (6 to 10) hours is more characteristic for homologous eruptions. The Sun rotates by about 0.6^0 in an hour ,so most successive CMEs from the same active region are separated by (4 to 6)^0. However ,the large spatial extent of CMEs makes the interaction of successive CMEs likely in those cases. The eruptions on April 29-May 2,1998 (AR 8210,SHINE campaign event) November(4- 5) ,1998 (AR 8375) , September(15-16),2000 (AR 9165 ,for these two events ,see for example[44]are good examples of multiple Earth-directed eruptions from the same active region. A particularly interesting succession of eruptions occurred in November (24-27) ,2000 , with six Earth directed eruptions from AR 9236 with in 60 hours. In this particular case,the high frequency of eruptions is related to the high rate of magnetic flux emergence[45]. It is also possible that eruptions from two adjacent active regions lead to the interaction of CMEs. When the delay between successive ejections is short enough or when a fast ejection is preceded by a much slower one ,interaction of CMEs can even be observed directly with coronagraphs. Such an example of two CMEs interacting in LASCO C3 field of view is shown in Figure 2.2. The interest in interacting CMEs quickly grew in the solar physics community after the first published report of two CMEs interacting in the LASCO C3 field of view[26]. This first direct detection was quickly followed by other [46].

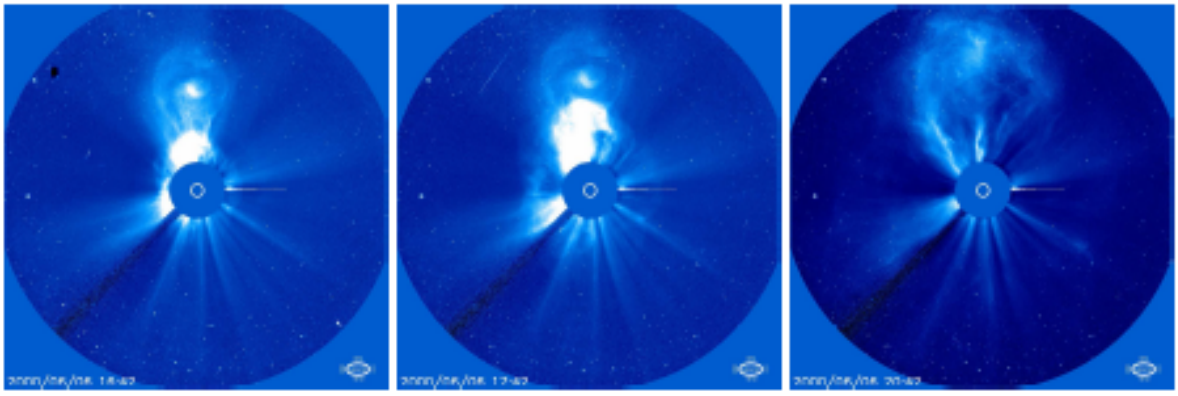

Figure 2.2: An example of CME "cannibalism" from LASCO C3

2.3.2 CME-CME Interaction and Radio Emission

The interaction of CMEs can produce various types of radio emissions ,such as types II and III radio bursts. Type II radio bursts are produced by non thermal electrons accelerated in magneto hydro dynamics shock propagating from low corona in to interplanetary space with the emission frequency slowly drifting from high to lower frequencies due to decreasing electron density encountered by shock in the corona[47]. Type II bursts are associated with shock waves in the solar corona ,while type III bursts are linked energetic electron streams. [48] investigated how coronal holes influence the structure and interactions of CMEs. They found that the presence of coronal holes could modulate the intensity of radio emissions resulting from CME-CME interactions. When CMEs interact ,their magnetic fields can reconnect ,leading to intensified magnetic fields and accelerated particles ,which enhance radio emissions. The dynamics of their interactions are complex and depend on the relative speeds and magnetic orientations of the CMEs .[41] presented observations of an extreme storm in interplanetary space caused by successive CMEs. They provided detailed analysis

of the interactions and their consequences ,including strong radio emissions. The high rate(6 day) of CME occurrence during solar maximum and the observed range of speeds ,one would expect frequent interaction between CMEs. Although interactions among shocks and ejecta are known to happen in the hemisphere[49] ,SOHO images and Wind/WAVES dynamic spectra provided direct evidence for CME interactions very close to the Sun[50, 18]. These interactions resulted in broad band non thermal radio enhancements in the decameter hectometric (DH) wavelength domain. Strengthening of the shocks when propagating through the dense parts of preceding CMEs and trapping of particles in the closed loops of preceding CMEs were suggested as possible mechanisms that increase the efficiency of particle acceleration[51]. A sudden radio enhancement occurred over an existing type II radio burst as seen in the Wind/WAVES dynamic spectrum of a DH type II burst. The radio enhancement is clearly non thermal emission and brighter than the associated type II burst. A very fast ,shock-driving CME (CME2 , 2657 kms^{-1}) approached a slower CME(CME1 ,600 kms^{-1}) and its dense core (CORE1). The radio enhancement occurred when CME2 reached a heliocentric distance of 18 ,close to the core of CME1. The 21:18 UT SOHO image shows that the CME2 and CORE1 are very close when the radio enhancement started. The radio emission lasted for about 40 min ,roughly the time taken by the CME-driven shock to traverse CORE1 (size 7). The high frequency edge of the type II burst was at 1 MHz when the interaction signature started with a high frequency edge of 3 MHz. A jump of 2 MHz in frequency would correspond to a density jump of 4 with respect to the ambient corona. This is also consistent with the appearance of CORE1 in white light.

2.3.3 Previous Studies of CME-CME Interaction

The first studies of the interaction of a shock wave with a magnetic cloud were done by [52]. The work by [53] was the first self consistent(and three dimensional) MHD simulation of the interaction of two CMEs from Sun to Earth. Due to the complex nature of complex ejecta ,it is not possible to use a simple model to fit the in-situ measurements ,with the possible exception of some multiple magnetic cloud structure. while several studies established that CME-CME interactions are likely to increase the impact on earth (geoeffectiveness) of individual CMEs [54]. Although the probability of CME-CME interaction in the corona and IP space is higher during periods of maximum solar activity ,when the CME occurrence can exceed the rate of 10 CMEs/day[55, 56]. The propagation of one CME and its interaction with the solar wind have been simulated since the 1990s by different groups in 2.5D and 3D[57, 58, 59]. The interaction of one CME and its front shock with the bimodal solar wind characteristic of solar minimum conditions is now fairly well understood.

Chapter 3

Data, Data Analysis and Results

3.1 Data and Data Selection

Radio observations in the Deca-Hecto metric range by radio and plasma wave experiment on board the Wind/WAVES spacecraft are taken from the online catalogue (http ://cdaw.gsfc.nasa.gov/CMElist/radio/wavestype2.html) [60]. The study period spans from (2009-2018) with some large data gaps and poor events. We verified the CME-CME interaction from (h-t)data in the field of view(FOV)of SOHO/LASCO , by over lapping of CMEs in position angle(PA)in SOHO/LASCO movies and enhancements from radio dynamic spectrum. The CME-CME interaction was further confirmed from different instruments by the over lapping in(PA) in the movies of Cor2 coronagraph on board STEREO. We adopted the DH type II burst data(Ts ,Te ,Fs ,and Fe) from the online Wind/WAVES type II catalog and the data corresponding to CMEs are adopted from the SOHO/LASCO CMEs catalog , maintained by NASAS CDAW data center online catalog (http ://.cdaw.gsfc.gov/CMElist[61, 27]). Out of the 47 CMEs , we have found only 32 potential radio-loud CMEs have possibly interacted in the Solar Cycle 24. We identify the main CME from the Coordinated

Data Analysis Workshop (CDAW) Data Center CME list. In this study ,we used the following criteria to identify the interacting events :

i)we included all pre and pri-CMEs with V>500 kms^{-1} , W>60^0 ,180<P.A.< 360^0 as selected by[62].

ii)pri-CMEs originating from the same region or close to the location of pre-CME.

iii) For the CME-CME interaction study we analyze white light images from the Solar Terrestrial Relations Observatory (STEREO-A; http://www.stereo.rl.ac.uk/HIEventList.html) SECCHI instrument suite.SECCHI consists of two coronagraphs ,COR1 and COR2,covering a plane of sky (POS) distance range up to 15 R ,and the heliospheric imagers (HI),HI1 and HI2,for distances > 15 R [63]. In conforming CME-CME interaction ,we have visually examined the movies($https://cdaw.gsfc.nasa.gov/movie/$) from CDAW for these events to show physical overlap. The CMEs location source were also taken from online Solar Geophysical Data (SGD) to identify eruption location. These radio-loud CME-CME interaction events were analyzed by python to show graphically. The properties of pri and pre-CMEs are listed below ,which are taken from the CDAW online data base.

The letters t_s ,t_e ,f_s and f_e refer to the start time (in UT) ,end time(in UT) ,starting frequency (in MHz) ,and the end frequency (in MHz)of the type II burst ,the Loc ,t ,W ,V ,a ,and describe both the pre and pri-CMEs ,time (in UT),width of the CME (in deg),speed of CME (in kms^{-1}) ,acceleration of CME (in ms^{-2}) ,interaction time in(UT),time duration in (min),and drift rate in ($MHzs^{-1}$,respectively.

A DH type II burst event on 2013 may 15 with on set time 06:35 UT is driven by pri-CME with the FAC2 $\sim$ 01:48 UT ,and the pre-CME is identified with FAC2$\sim$23:12 UT on 2013 may 14 and for the DH type II burst event on 2011 August 14 with onset

yy-mm-dd	DH type II burst						Source Location	Preceding CMEs					Primary CMEs					CMEs T_{in}	Time duration	Interaction height	Dirft rate
Events	D_S	T_S UT	D_e	T_e (UT)	F_s (MHz)	F_e MHz	SL	D_S	T UT	W deg	V Km s^{-1}	A ms^{-2}	Ds	T UT	W deg	V kms^{-1}	A ms^{-2}	UT	min	Rs	MHz/s
2011-03-07	03/07	20:00	03/07	08:30	16	0.2	N31W53	03/07	14:48	261	698	-8.3	03/07	20:00	360	2125	-63.10	20:48	48	10.7	0.38
2011-08-04	08/04	04:15	08/04	17:00	13	0.06	N19W36	08/04	14:00	360	610	-12.2	08/04	04:12	360	1315	-41.0	05:12	57	11.4	0.28
2011-08-08	08/08	18:00	08/08	20:10	6	0.4	N16W61	08/08	23:12	74	1070	-87.1	08/08	18:12	237	1343	-42.3	19:12	72	9.46	0.77
2011-08-09	08/09	08:20	08/09	08:35	16	0.4	N17W69	08/09	03:48	141	1146	-21.9	08/09	08:12	360	1610	-40.6	09:20	60	13.4	17.3
2011-09-22	09/22	11:05	09/22	24:00	14	0.07	N09E89	09/22	08:48	53	508	10.9	09/22	10:48	360	1905	-68.30	12:00	55	16.5	0.29
2012-03-07	03/07	01:00	03/07	19:00	16	0.03	N17E27	03/07	01:30	360	1825	-160.9	03/07	00:24	360	2684	-160.9	01:48	48	18.4	0.24
2012-07-19	07/19	05:30	07/19	06:20	5	0.6	S13W88	07/19	06:24	360	873	-10.9	07/19	05:24	360	1631	-8.00	6:48	06	3.7	1.46
2013-05-13	05/13	16:15	05/13	19:10	16	0.3	N11E85	05/13	17:24	149	849	-0.1	05/13	16:07	360	1850	-76.6	17:36	81	10.3	1.58
2013-05-15	05/15	01:49	05/15	07:57	16	0.23	N12E64	05/15	23:12	121	667	-11.1	05/15	01:48	360	1366	-52.1	02:24	35	8.6	0.71
2013-05-22	05/22	13:10	05/22	06:00	16	0.15	N15W70	05/22	08:48	210	687	16.8	05/22	13:25	360	1466	-13.2	14:00	50	9.8	0.61
2013-10-25	10/25	04:41	10/25	11:51	14	0.2	N08W71	10/25	08:12	360	587	-13.7	10/25	15:12	360	1081	-45.2	16:36	88	12.6	0.59
2013-10-28	10/28	15:08	10/28	22:32	16	0.2	S06E69	10/28	02:24	360	695	-12.1	10/28	04:48	156	1201	-25.2	05:36	55	8.5	0.53
2013-12-12	12/12	03:55	12/12	21:30	12	0.07	S23W46	12/12	06:24	240	723	-4.9	12/12	03:36	276	1002	-15.3	07:48	225	5.7	0.18
2014-02-20	02/20	08:05	02/20	08:29	12	7.7	S15W73	02/20	01:25	143	646	2.8	02/20	08:00	360	948	-9.50	09:24	79	9	2.98
2014-05-07	05/07	16:24	05/07	23:18	16	0.2	S11W100	05/07	11:48	331	811	-9.5	05/07	16:24	360	923	-22.10	17:24	72	10.2	0.58
2014-09-10	09/10	17:45	09/10	12:00	14	0.1	N14E02	09/10	17:24	134	1071	-61.8	09/10	18:00	360	1267	-51.6	19:00	75	10.9	0.67

Figure 3.1: List of radio-loud CME-CME Potential interactions in Solar Cycle 24 in the years 2009 to 2018

time 04:15 UT is driven by pri-CME with the FAC2 $\sim$ 04:12 UT ,and the pre-CME is identified with FAC2 $\sim$ 14:00 UT on 2011 August 13 from the neighboring source region which is from the CDAW/CME catalog. The pre-CME in the event on 2012 may 17 can not be identified in the LASCO field of view due to the data gap of LASCO CME catalogue.

3.2 Data Analysis

We analyzed statistically the data of 32 potential radio-loud interacting CMEs in SC 24 ,which are derived from CDAW/NASA observatories group particular with the catalogue (http : //cdaw.gsfc.nasa.gov/CMElist/radio/wavestype2.html) and the CME

data is downloaded from SOHO/LASCO CME catalog (https : //cdaw.gsfc.nasa.gov/CMElist/) and in conforming CME-CME interaction,we have visually examined the movies(https : //cdaw.gsfc.nasa.gov/movie/) from CDAW for these events to show physically overlap. The data set for this statistical study is composed of 16 DH component associated pri-CMEs and 16 preceding CMEs in the Solar Cycle 24 during 2009 to 2018. The analysis starts with describing kinematic properties of Pre and pri-CMEs ,source location of pri and pre-CMEs ,CME-CME interaction time and duration of interaction time ,interaction height , and drift rate. We describe these radio-loud CME-CME interaction events were analyzed by python to show graphically.

3.3 Results

In this section we analyzed the 32 radio-loud CME-CME Potential interactions in the Solar Cycle 24 events derived from remote solar observations. In particular ,we investigate the possible CME-CME potential interaction events in solar cycle 24 ,the relationship between the frequency characteristics of DH type II radio burst counter part CMEs ,the pri and pre-CMEs linear speed ,acceleration,angular width ,source location of pri and pre-CMEs ,CMEs interaction time ,time duration ,and CMEs interaction height.

3.3.1 Illustrative Examples

As an illustration of our analysis,a CME was observed by LASCO C2 coronagraph at 8:48 UT at a height of 2.73 Ro (where ,one solar radius is 696000 km) , and it was well observed as a partial halo (210^0) CME with sky plane speed of 687 kms^{-1} and

an acceleration of 16.8 ms^{-2}. This CME is considered as pre-CME. Following this , a halo-CME with speed v (1466) kms^{-1} was observed by LASCO C2 at 13:25 UT at a height of 4.63 Ro. This CME ,called a pri-CME,was reported to decelerate as -13.2 ms^{-2}. Around 14:00 UT , the pri-CME interacted with the pre-CME. The height-time data of pre and pri-CMEs were linearly fitted and the interaction height was estimated to be ∼18 Ro. The start time of DH type II bursts was very close at 13:10 UT as revealed from the Wind/WAVES dynamic spectra. The primary halo CME merged with the slow pre-CME and the pri-CME traced throughout the LASCO field of view.

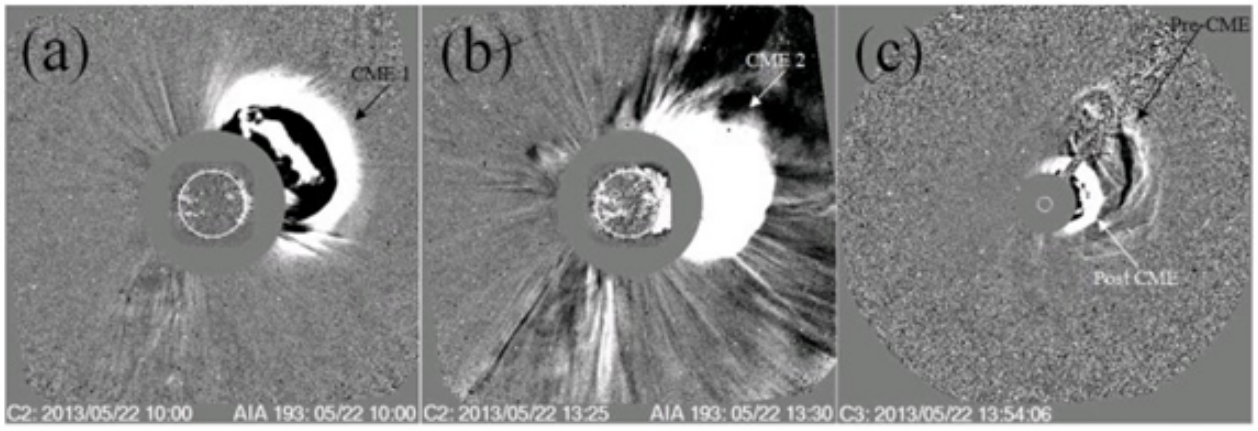

Figure 3.2: RL CME-CME interaction was observed on 2013 May 22 in LASCO C2 and C3 Field of view. This RL CME interacted with pre-CME on the same date. The position of the pri and pre-CMEs are indicated by the black and white arrows in panel c.

3.3.2 Kinematic properties of Pri and pre-CMEs

We compiled the three basic attributes (speed , angular width , and acceleration) of the pri and pre-CMEs. Both CMEs speeds are obtained by a linear fit to the

height-time measurements in the sky plane. Figure 3.3 illustrates the distribution of speed of both CMEs during solar cycle 24 (2009 to 2018). The graph shows that there are more number of pre and pri-CMEs in the range (500 to 1000) kms^{-1} and (1000 to 1500)kms^{-1},respectively. The average speed of pri and pre-CMEs have found to be 1482.3 kms^{-1} and 841.7 kms^{-1} ,respectively. Fourteen out of 16 pri-CMEs and five out of 16 pre-CMEs (87.5% and 31.25%)of them were speeds greater than 1000 kms^{-1} , two Out of 16 pri-CMEs and eleven out of 16 pre-CMEs (12.5% and 68.75 %) are with speed ranging between 500 and 1000 kms^{-1} , eight out of 16 pri-CMEs and four out of 16 pre-CMEs (50% and 25 %) were with speeds ranging 1000 and 1500 kms^{-1} , four out of 16 pri-CME and one out of 16 pre-CMEs(25 % and 6.25 %) were speeds ranging between 1500 and 2000 kms^{-1} , one out of 16 pri-CMEs (6.25 %) with speeds ranging between 2000 and 2500 kms^{-1} ,and one out of 16 pri-CMEs (6.25%) were with speeds greater than 2500 kms^{-1}. The acceleration of pri and pre-CMEs were negative or decelerated ,and they were Consistent with their high speeds ,87.5% and 31.25% of both CMEs. The positive acceleration for the pre-CME is due to the uncertain values at the tail.Figure 3.3 illustrates the angular width of both CMEs ranges from 156^0 to 360^0 and $(74\text{-}360)^0$, with average width of 334.3^0 and 228.6^0. Most (81.3%) of the pri-CMEs are full halos (w=360^0) where as the pre-CMEs(37.5%) of the total 16 events are full halos(w=360^0). When we included the partial halos of pri and pre-CMEs (>120^0) to the percentage of full halos ,the result become increased to 100% and 93.25% respectively ,except the one(1 pre-CME is non halo).

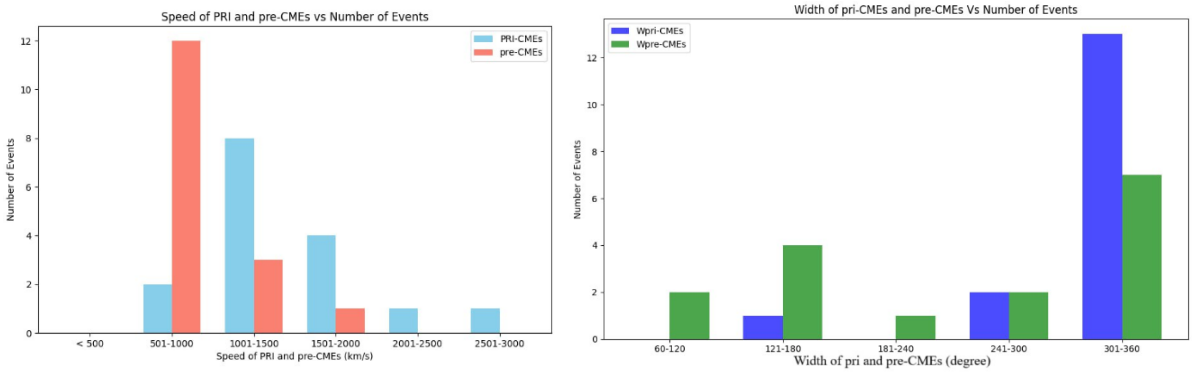

Figure 3.3: distribution of speeds and widths of pre and pri-CMEs Vs number of events

3.3.3 source location of pri and pre-CMEs

Figure 3.4 presents the source location of 32 potential radio-loud interacting CMEs (pri and pre-CMEs) events. Twelve Out of 32 events (37.5 %) of the radio-loud CME-CME potential interaction in SC 24 are found in the North West regions. Ten out of 32(31.25 %) were comes from the North East. Eight out of 32 (25 %) of the events originated from the South West region , and Two out of 32 (6.25 %) comes from South East regions. It is clearly seen that from the graph most of the radio-loud CME-CME potential interaction in sc 24 are from the western hemisphere.

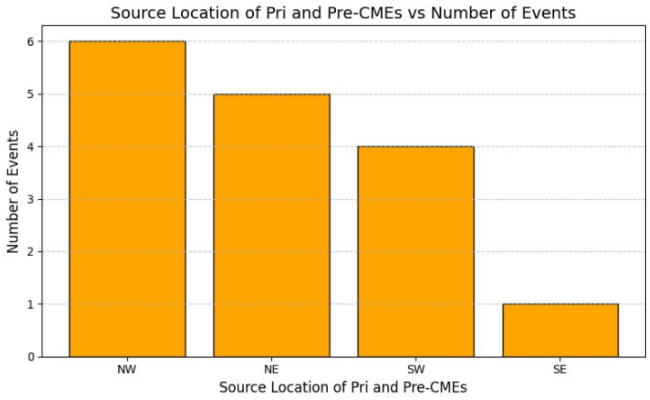

Figure 3.4: Source location of Pri and Pre-CMEs Vs number of events

3.3.4 Frequency Ranges of the associated DH type II burst counter parts

Figure 3.5 shows the distributions of starting and ending frequency events. starting frequency of the DH component emission is a special feature for determining the height of the shock and giving a potential interaction for forecasting space weather events. The starting frequency of DH component varies from 5 MHz to 16 MHz. Eight events out of the 16 DH component emission associated CMEs were linked to the starting frequencies in the range of 16 MHz (50%) , six out of the 16 (37.5 %) have frequency range were linked to 12 MHz and 14 MHz,and the rest 2 out of 16 events (12.5 %) at frequency of 5 MHz and 6 MHz were linked for the starting frequency of the DH type II radio burst , and concerning to the ending frequency 6 out of the 16(37.5 %) where have frequency range were linked to 0.2 and 0.3 MHz,4 out of the 16 events (25 %)frequency range were linked to 0.4 and 7.7 MHz , and 5 out of the 16 events(31.25 %)frequency range were linked to 0.06 and 0.1 MHz for the ending frequency of DH type II bursts. The starting and ending frequencies indicate that the height at which the plazma radio emission from the shocks becomes visible. We found the average of start and end frequencies (13.6 MHz and 10.8 MHz) , respectively. The higher starting frequency of DH type II bursts for SC 24 is thought to contribute to shock formation at lower heights. The distribution of the start and end frequencies for all radio-loud CMEs associated events in SC 24 is shown in Figure 3.1 in the second column. Drift rate ($\frac{df}{dt}$) is a displacement of the peak in frequency per unit time. The absolute value of rate decreases with decreasing in frequency. It is determined by taking the start time to end time and start frequency to the end frequency of the solar burst DH Type II. With a low drift rate will leads to low velocity of the event to

occur. Drift rate of the solar radio burst type II was defined as: Drift rate ,$\frac{df}{dt}=\frac{fe-fs}{te-ts}$ =MHzS^{-1} , Where f$_e$ is frequency of end time ,f$_s$ is frequency of start time ,t$_e$ is end time ,t$_s$ start time.

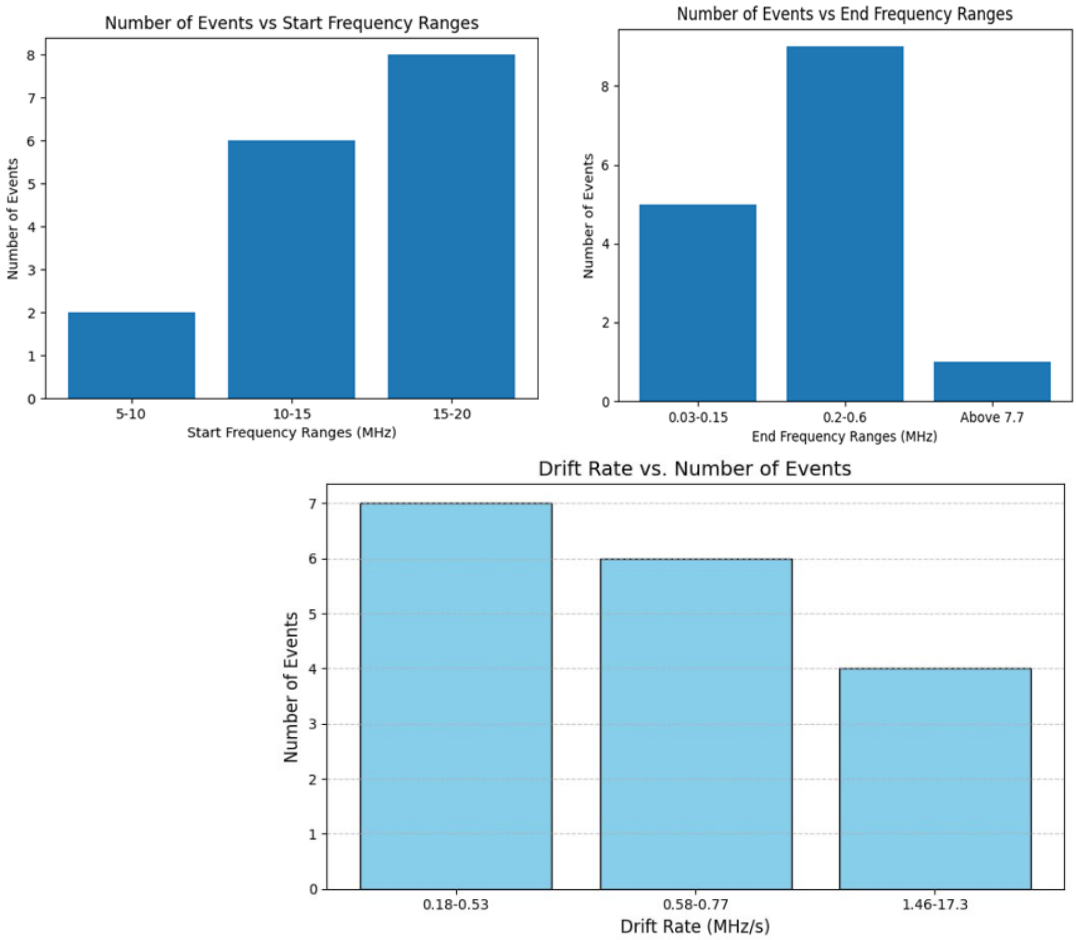

Figure 3.5: distribution of starting , ending frequencies,and drift rate Vs number of events

3.3.5 CMEs time duration and interaction heights

The distribution of time duration and interaction height between the first detection times of pri and pre-CMEs is plotted in Figure 3.6. We found that 6.25% were with

time duration ranging between 0 to 35 minute , 25% were with time duration ranging between 35 to 70 minute , 15.63% were with time duration ranging between 70 to 105 minute , and one event 3.13% is above 140 minute. While , 25% were with interaction height ranging between 3.7 to 10.2 Ro , 18.75% were with interaction height ranging between 10.3 to 13.4 Ro , 6.25% are with interaction height ranging between 16.5 to 18.4 Ro., and the average time duration and interaction height are found to be ∼34.6 minutes and ∼5.3 Ro. Their interacting time and height are obtained by clicking interaction time and interaction height of the potential radio-loud CME-CME interactions in SC 24 is being estimated from the white light image of SOHO/LASCO running difference imagers using the movies. It appears that the time duration increases when the interaction occurs at large distances. In all the above analysis ,the interaction was validated using LASCO white light running difference images. Perhaps the CME interaction began at a lower height ,which is obscured by the occulter disk. Because of the time gap (12 minutes) between LASCO image sequences/observations ,we may miss the exact interaction height.

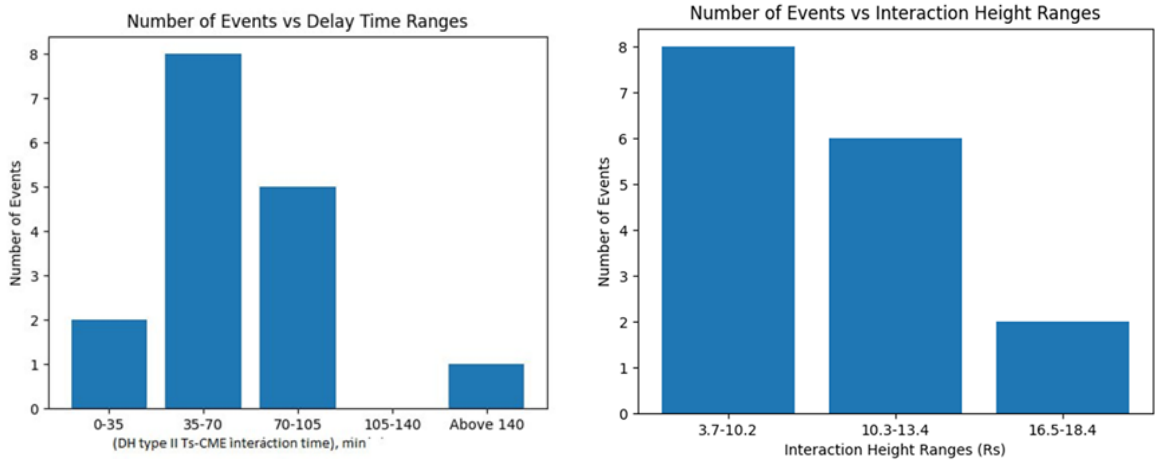

Figure 3.6: Distribution of time duration and interaction height of pri and pre-CMEs Vs number of events

Chapter 4

Discussion and Conclusion

4.1 Discussion

We studied the CME spans have to overlap and their trajectories need to intersect in order to realize an interaction with in the range of the IP medium accessible to the WAVES RAD2 receiver in the DH domain. The DH domain roughly corresponds to about 3 to 10 Rs , for typical density distribution in the outer solar atmosphere[26]. The DH type II bursts are indicative of shocks in the outer corona driven by fast and very wide CMEs. During solar maximum when the activity is the largest , one would expect more interactions. The typical interaction scenario seems to be a slow CME followed by a fast CME. We found that the distribution of speeds ,widths ,and accelerations of pre and pri-CMEs are shown in the Figure 3.3. The average speed and width for pri and pre-CMEs were (1482.3 ,841.5) kms^{-1} and (334.3 ,228.8)^0 ,respectively. These speeds were similar to the average speed of pre and pri-CMEs (700 kms^{-1}) and (1480 kms^{-1}) which is reported by [26]. We found that (81.3 %) were full halo pri-CMEs , while (18.8%) were partial halo pri-CMEs ,where as (37.5

%) were full halo pre-CMEs ,(56.3 %) were partial halo pre-CMEs , and one pre-CME is non hallo event was found in the limb (N16W61 on 2011 August 08) arrive at Earth with enhanced North ward component of the magnetic field. while limb halos only impact Earth with their flanks and hence are less geoeffective. This result was consistent with the result of[64] in which they reported that faster CMEs (greater than 900 kms^{-1}) are mostly decelerated. Therefore , the average speed of the pri and pre-CMEs were much greater than the average speed of general CMEs 470 kms^{-1}[65].

Figure 3.4 shows the distributions of source location of radio-loud pri and pre-CMEs , we found that 37.5% are from North West ,25% are from North East ,31.25% are from South West , 6.25% are from south east hemisphere. It is clearly seen that most of the pri and pre-CMEs are located in the western hemisphere , and the reason is that Western CMEs are magnetically well-connected to the Earth. Figure 3.5 shows the distributions of starting and ending frequencies. The starting frequency of the DH component emission is a special feature for determining the height of the shock and giving a potential interaction for forecasting space weather events. The starting and ending frequencies of DH component varies from 5 MHz to 16 MHz and 0.03 MHz to 7.7 MHz. We found that the average of start and end frequencies (13.6 MHz and 10.8 MHz) , respectively. The starting and ending frequencies indicated that the height at which the plazma radio emission from the shocks becomes visible. The higher starting frequency of DH type II bursts for SC 24 is thought to contribute to shock formation at lower heights. Drift rate of the solar radio burst type II was defined as:Drift rate , $\frac{df}{dt} = \frac{fe-fs}{te-ts}$=(MHzS^{-1} ,Where f_e is frequency of end time,f_s is frequency of start time , t_e is end time , t_s start time. With a low drift rate will leads to low velocity of the event to occur. The distribution of drift rate in $MHzs^{-1}$ of DH

type II bursts associated with pri-CMEs is shown in figure 3.1 in the last column of the table. The average drift rate is found to be 1.82 MHzs^{-1}.

Figure 3.6 shows the distributions of time duration and interaction height of CMEs. We found the interacting time and height are obtained by clicking interaction time and interaction height of the potential radio-loud CME-CME interactions in solar cycle 24 is being estimated from the white light image of SOHO/LASCO running difference imagers using the movies. And the average time duration and interaction height of pri and pre-CMEs are found to be ∼34.6 minutes and ∼5.3 Ro ,respectively. The average interaction height of pri and pre-CMEs were three times less than 21 Ro reported by[66]. It appears that the time duration (duration of interaction time) increases when the interaction height occurs at large distances. In all the above analysis ,the interaction was validated using LASCO white light running difference images. Perhaps the CME interaction began at a lower height , which is obscured by the occulter disk. Because of the time gap (12 minutes) between LASCO image sequences/observations ,we may miss the exact interaction height.

4.1.1 Conclusion

We analyzed 32 potential radio-loud CMEs detected by SOHO/LASCO and DH type IIs observed at Wind/WAVES space craft. For the CME-CME interaction study we analyze white light images from the Solar Terrestrial Relations Observatory (STEREOA; http://www.stereo.rl.ac.uk/ HIEventList.html) SECCHI instrument suite and in conforming CME-CME interaction,we have visually examined the movies (https ://cdaw.gsfc.nasa.gov/movie/) from CDAW for these events to show physical overlap. The interaction results in the enhancement of radio emission for

the duration corresponding to the transit time of the fast CME shock through the core of the preceding slow CME. The interaction severely affects the trajectory of the preceding CME core. The interaction between CMEs have important implications for space weather applications: (1) the interaction causing deflection can explain the lack of manifestations of some Earth-directed CMEs at 1 AU ,and (2) it can explain composition anomalies of some CMEs at 1 AU[19]. A set of 32 potential interacting radio loud CMEs ejected from the nearby active region in the same quadrant and associated with DH components are identified during the period 2009 to 2018 as well as their properties are analyzed. These events are collected based on our selection criteria. The pri and pre-CMEs and their interactions are identified using LASCO images of SOHO ,STEREO images of SECCHI , and their height-time diagrams.

Results from this analysis were:

i) Pri-CMEs are much faster and wider than the pre-CMEs

ii) From the observational data of speed and width of pre and pri-CMEs , it is Found that the pre-CMEs are found to be less energetic than the pri-CMEs.

iii)the time duration increases when the interaction height occurs at large distances.

In our investigation ,we found that the interaction time and interaction height of the potential radio-loud CME-CME interactions in SC 24 is being estimated from the white light image of SOHO/LASCO and Solar Terrestrial Relations Observatory (STEREO-A;http://www.stereo.rl.ac.uk/ HIEventList.html) SECCHI instrument suite running difference imagers using the movies. The average speed of pri-CMEs(1481.3 kms^{-1}) is found to be much greater than the average speed of Pre-CMEs (841.6 kms^{-1}) , similarly the average angular width of the pri-CMEs(334.3^0) are found

to be greater than the the average angular width of pre-CMEs (254.6^0),respectively. The percentage of halo pri-CMEs occurrence were too high (81.3%) than the percentage of halo pre-CMEs (37.5%) in the Solar Cycle 24. [67] most of the pri-CMEs were hallo type CMEs and much faster than the pre-CMEs. And we found also the average (start frequency ,end frequency , drift rates) of the DH component emission ,the time duration and interaction height of pri and pre-CMEs (13.6 MHz ,10.8 MHz ,1.82 $MHzs^{-1}$) ,($\sim$34.6 min , and $\sim$5.3 Ro) , respectively.

Space weather is mainly caused by the Sun because of the variability in its mass and photon emissions on various time scales. CMEs and the solar wind carry the coronal magnetic field in to the heliosphere. CMEs propagate in to the solar wind and drive shocks; the shocks accelerate SEPs. Flares also accelerate particles , but generally over shorter duration and to lower intensity levels. When CMEs arrive at Earth ,they interact with Earth's magnetosphere causing geomagnetic storms ,which have multiple of effects from the magnetosphere to the ground[27]. Understanding the dynamics of radio-loud CMEs and their interactions helps in predicting space weather events ,which can affects satellite operations ,communication systems,and power grids on Earth[25, 26]. By elucidating how these CMEs influence geomagnetic storms , the study contributes to better preparedness and response strategies for mitigating the adverse effects of space weather. The main reason why we need this type of research is that making better space weather prediction is crucial for the stability of our strongly technology dependent society.

Bibliography

[1] Assgeir Brekke. *Physics of the upper polar atmosphere.* University of Troms, Norway., 1997.

[2] G. M.Kivelson and C. T.Russell. *Introduction to Space Physics.* Cambridge University press, UK, 1995.

[3] K.R.Lang. *the Cambridge Encyclopedia of the Sun.* Cambridge University Press, 2001.

[4] A.Bouvier and M.Wadhwa. *The age of the Solar System reddened by the oldest Pb-Pb age of a meteoritic inclusion.*, volume 637. 2010.

[5] K.Petrovay and U.R.Christensen. the magnetic sun: Reversals and long-term variations. *Space Sci.Rev.*, 155:371, 2010.

[6] T.Tsega. *New Insights into the Relation between Coronal Mass Ejections and Non thermal Radio Emissions.* PhD thesis, PhD thesis,Addis Ababa University,Ethiopia., 2016.

[7] Tilaye Tadesse Asfaw. *nonlinear force-free reconstruction of the coronal magnetic field with advanced numerical methods.* PhD thesis, PhD thesis, Addis Ababa University, Ethiopia., 2011.

[8] G.E.Hale. On the probable existence of a magnetic field in sun-spots. *ApJ*, 28:315, 1908.

[9] P.Zeeman and B.Winawer. the magnetic separation of absorption lines in connection with sun-spot spectra. *ApJ*, 32:329, 1910.

[10] J.T.Mariska. *The Solar Transition Region*. Cambridge University press., UK, 1993.

[11] R.Schwenn and E.Marsch, editors. *Physics of the Inner Heliosphere I. Large-Scale Phenomena*, volume 14. Springer-Verlag, New York, 1990.

[12] Calvin J. Hamilton. *the solar system*. 2009.

[13] Linghua Wang. *Solar impulsive energetic electron events (1-17)*. university of California, http://escholarship.org/UC/item/33w5q946 http://en.m.wikipedia.org/wiki/ solar flare (June 2011), 2009.

[14] E.R.Priest. *Solar flare magneto hydrodynamics*. Gordon and Breach Science publisher, 1981.

[15] M.Moldwin. *An introduction to space weather*. Cambridge University Press, New York, 2008.

[16] W.D.Pesnell, B.J.Thompsom, and P.C.Chamberlin. "the solar dynamics observatory.". *Solarphysics.*, 291:5–6, 2016.

[17] N.Gopalswamy, H. Xie, S.Akiyama, P.Mkel, and S.Yashiro. Major solar eruptions and high energy particle// events during solar cycle 24, aip conference proceedings. 66:104, 2014.

[18] N.Gopalswamy, S.Yashiro, M. L.Kaiser, R.A.Howard, and J.-L.Bougeret. *Geophys.Res. Lett*, 28(8):DOI:10.1029/2001GL013606, 2002a.

[19] M.Temmer, B.Vrnak, T.Rollett, B. Bein, C.A.de koning, Y.Liu, and E.Bosman et al. *Astrophys.J.*, 749:57, 2012.

[20] S.Prasanna Subramanian and A.Shanmugaraju. Study of interacting cmes and dh type ii radio bursts. *Astrophys.Space Sci.*, 344:305–312,DOI: 10.1007/s10509–012–1347–4, 2013.

[21] G. E.Brueckner, R. A.Howard, and M.J.Koomen et al. *Sol.Phys.*, 162:357, 1995.

[22] M.L.Kaiser, T.A.Kucera, J.M.Davila, O. C.St. Cyr, M.Guhakurta, and E.Christian. The stereo mission: An introduction. *Space Sci. Rev.*, 136:5, 2008.

[23] R.A.Howard, J.D.Moses, and A.Vourlidas et al. *Space Sci.Rev.*, 136:67, 2008.

[24] N.Gopalswamy. *Coronal Mass Ejections: a Summary of Recent Results, in Proc.20th Slovak Nat. Solar Phys. Meeting, edited by I. Dorotovic*. Slovak Central Observatory, UK, 2010.

[25] A.O.Benz and S.Krucker. "the radio emission from solar flare and cmes.". *space science reviews*, 101(1):297–314, 2002.

[26] N.Gopalswamy, A.Lara, S.Yashiro, M.L.Kaiser, and R.A.Howard. "predicting the1-au arrival times of cmes.". *Journal of Geophysical Research,Space physics*, 106(A12):29207–29218,.doi:10.1029/2001JA000177, 2001.

[27] N.Gopalswamy. *Coronal mass ejection and space weather. In Climate and Weather of the Sun-Earth System (CAWSES).* selected papers from the200750Kyoto Symposium, eds. T.Tsuda and R.Fujiiand K.Shibata and M. A.Geller, Terrapub and Tokyo., 2009a.

[28] N.Gopalswamy. X-ray and microwave signatures of coronal mass ejections, in solar physics with radio observations, edited by t. bastian and n. gopalswamy and and k. shibasaki. *NRO Report No*, 479:141, 1999.

[29] N.Gopalswamy, Z.Mikic, D.Maia, D. Alexander, H.Cremades, P. Kaufmann, D.Tripathi, and Y.-M.Wang. The pre-cme sun. *Space Sci. Rev.*, 123:303–339, March 2006.

[30] N.Gopalswamy and S.Yashiro. *ApJ*, 736:L17, 2011.

[31] R.A.Howard, D.J.Michels, Jr.N. R.Sheeley, and M.J Koomen. The observation of a coronal transient directed at earth. *Astrophys.J.*, 263:L101, 1982.

[32] N.Gopalswamy, S.Yashiro, M.L.Kaiser, R.A.Howard, and J.-LBougeret. Characterstics of coronal mass ejections associated with long-wavelength type ii radio bursts. *J.Geophys.Res.*, 106:29219, 2001a.

[33] N.Gopalswamy. Geoeffectiveness of halo coronal mass ejections. *J.Geophys. Res.*, 112:A06112, 2007.

[34] S.Yashiro, N.Gopalswamy, S.Akiyama, G.Michalek, and R.A.Howard.

[35] C.J.Schrijver et al. "understanding the solar cycle: Active regions and coronal mass ejections.". *Nature*, 515(7525):226–229, 2014.

[36] B.T.Tsurutani et al. "c mes and their effects on earth's magnetosphere.". *Geophysical Research Letters*, 33(14):L14105, 2006.

[37] S.Yashiro et al. "a catalog of large cmes from 1996 to 2006.". *The astrophysical journal*, 651(2):1250–1264, 2006.

[38] S.J.Bame et al. " solar cycle variation of cme sources.". *solar physics*, 61(2):203–2014, 1979.

[39] D.F.Webb, J. T.Nolte, C. V.Solodyna, and P.McIntosh. *Solar Phys.*, 1978.

[40] A.Bhatnagar. Solar mass ejections and coronal holes. *Astrophys .Space Sci.*, 243:105, 1996.

[41] Y.D.Liu, J.G.Luhmann, P.Kajdic, E.K.J.kilpua, N.Lugaz, N.V.Nitta, and S.D.Bale. "observation of an extreme storm in interplanetary space caused by successive cmes.". *nature of communication*, 5:3481, 2014.

[42] C.Shen, Y.Wang, Z.Pan, B.Miao, P.Ye, S.Wang, and R.Xie. "full hallo cmes :arrival at earth.". *Journal of geophysical research:spacephysics*, 11997:5107–5116, 2014.

[43] V. Peinhar, M. Temmer, and A.M.Veronig. Asymmetry in the cme-cme interaction process for the events from 2011 february 14-15. *Journal of geophysical research:spacephysics*, 2014.

[44] Noe E.R.Lugaz. *Numerical investigation of coronal mass ejection interacting in the inner helliospher*. PhD thesis, atmospheric and space science, 2007.

[45] N.V.Nitta and H.S.Hudson. Recurrent flare/cme events from an emerging fluxregion. *Geophys. Res. Lett.*, 28:3801–3804, 2001.

[46] M. J.Reiner, A.Vourlidas, O. C. S. Cyr, J.T.Burkepile, R.A.Howard, M. L. Kaiser, N.P.Prestage, and J.-L. Bougeret. Constraints on coronal mass ejection dynamics from simultaneous radio and white light observations. *Astrophys.J.*, 590:533–546, 2003.

[47] proffesor Rami Vainio. *investigation of properties SEPs and geomagneticstorms related to CMEs*. PhD thesis, University of Turku, 2019.

[48] P.Makela, N.Gopalswamy, S.Akiyama, H.Xie, and S.Yashiro. "coronal hole influence on the observed structure of interplanetary cmes.". 284(1):59–75, 2013.

[49] L.Burlaga, K.W.Behannon, and L.W.Klein. *J.Geophys. Res*, 92:5725, 1987.

[50] Gopalswamy N.and S.Yashiro, M. L.Kaiser, R. A. Howard, and J.-L. Bougeret. *Astrophys. J.*, 548:L91, 2001c.

[51] N.Gopalswamy et al. *Astrophys.J.*, 572:L103, 2002b.

[52] M.Vandas, S.Fischer, M.Dryer, Z.Smith, T.Detman, and A.Geranios. Mhd simulation of an interaction of a shock wave with a magnetic cloud. *J.Geophys.Res.*, 102:22295–22300, 1997.

[53] N.Lugaz, W.B.Manchester, and T.I.Gombosi. Numerical simulation of the interaction of two coronal mass ejections from sun to earth. *Astrophys.J.*, 634:651–662, 2005b.

[54] N.lugaz, M.Temmer, Y.wang, and C.J.farrugia. *soph*, 292:64, 2017.

[55] S.Yashiro, N.Gopalswamy, G.Michalek, O.C.and S.P. Plunkett St.Cyr, N.B. Rich, and R. A.Howard. *J. Geophys. Res.*, 109:7105, 2004.

[56] E.Robbrecht, D.Berghmans, and R.A.M.VanderLinden. *APJ*, 691:1222, 2009.

[57] D.Odstr?cil and V. J. Pizzo. Three-dimensional propagation of cmes in a structured solar wind flow: 1.cme launched within the streamer belt. *J.Geophys. Res*, 104:483–492, 1999.

[58] P.Riley, J. A. Linker, and Z. Mikic. An empirically-driven global mhd model of the solar corona and inner heliospher. *J.Geophys.Res*, 106:15889–15902, 2001.

[59] W. B.Manchester, T. I. Gombosi, I. Roussev, A. Ridley, D. L. De Zeeuw, I. V. Sokolov, K. G. Powell, and G. Toth. Modeling a space weather event from the sun to the earth: Cme generation and interplanetary propagation. *J. Geophys. Res*, 109:2107–+, 2004b.

[60] N.Gopalswamy, p.Makela, and S.Yashiro. *Sun and Geospher*, 14:111,Dol:10.31401, 2019.

[61] N.Gopalswamy. A global picture of cmes in the inner heliosphere, in assl . : The sun and the heliosphere as an integrated system, edited by g. poletto,and s. t. suess. 317:201–+, 2004.

[62] A.Vourlidas. do interacting coronal mass ejections play a role in solar energetic particle events??.

[63] M.Temmer et al. 'characteristics of kinematics of a coronal mass ejection during the 2010 august 1 cme-cme interaction event'. pages 1–29, 2010.

[64] M Bendict Lawrance, A.Shanmugaraju, and Sprasanna Subramamian. investigation of slow and fast cmes and their associated activities in sc 24. *Indian journal of radio and space physics*, 44:113–121, 2015.

[65] N.Gopalswamy. Consequences of coronal mass ejections in the heliosphere. *Sun and Geosphere*, 1(2), 2006b.

[66] N.Gopalswamy, S. Yashiro, G.Michalek, M.L.Kaiser, R. A. Howard, D. V. Reames, R.Leske, and T.von Rosenvinge. Interacting coronal mass ejections and solar energetic particles. *Astrophys.Journ. Lett*, 590:L103–L107, 2002.

[67] D.V.Reams. particle acceleration at the sun and the heliospher. *J.space sci.rev.*, 30:413, 1999.